Gulf of Mexico Gas Hydrate Joint Industry Project Leg II:
Alaminos Canyon 21 LWD Operations and Results

Gilles Guerin[1], Ann Cook[1], Stefan Mrozewski[1], Timothy Collett[2], & Ray Boswell[3]

Introduction

Two holes, Alaminos Canyon 21-A (AC 21-A) and Alaminos Canyon 21-B (AC 21-B), were drilled in the Gulf of Mexico Alaminos Canyon Block 21 within the Diana sub-basin to delineate potential gas hydrate accumulations in a shallow, turbidite channel/lobe complex. The targets were thick sand reservoirs encased in clay about 600 ft below the seafloor. The seismic signature of the target sands indicated higher velocities than in the surrounding clay, possibly because of the occurrence of gas hydrate. A complete assessment of the Alaminos Canyon 21 sites and a full description of the drilling operations are provided in Frye *et al.* (2009) and Collett *et al.* (2009).

Operations

Logging-while-drilling (LWD) operations at the Alaminos Canyon Block 21 Site were conducted using a state of the art bottom hole assembly (BHA), including the Schlumberger MP3, geoVISION, EcoScope, sonicVISION and PeriScope tools. For a detailed description of the BHA, of each tool and of the tool measurements, see Mrozewski *et al*. (2009).

Hole AC 21-A

After tagging the seafloor at a driller's depth of 4940 ft below rigfloor (fbrf), Hole AC 21-A was spudded at 05h00 on May 3, 2009. Following a protocol designed to maintain good conditions at the top of the hole (Collett *et al*., 2009), the first ~60 ft below seafloor (fbsf) were drilled while circulating 200 gallons of sea water per minute (gpm) and rotating the drill bit at only 15 rotations per minute (rpm). These rates were gradually increased to ~250 gpm and ~55 rpm at 60 fbsf, and maintained until the entire LWD tool string was in the hole (~170 fbsf). At this point, flow rate was increased to 350 gpm to activate all tools, the bit rotation rate was set at about 90 rpm, and the rate of penetration (ROP) to ~300 ft/hr.

Drilling continued smoothly with weighted sweeps of drilling fluid and water every other stand (60 ft of drill pipe in this configuration) until 500 fbsf when ROP was reduced to 170 ft/hr and rotation was increased to ~110 rpm for the target zone of interest. Starting at 750 fbsf, the downhole bit rotation rates became increasingly erratic. At 900 fbsf, ROP was returned to 330 ft/hr and remained constant until the total depth of 1760 fbsf was reached at 17h00 on May 3. The hole was not displaced with heavy drilling fluid because the bottom of the hole had been drilled with a 10.5 gpm drilling fluid. An LWD downlink was performed to slow the tools' record rates before the BHA was pulled out of hole and suspended in open water at 21h00 ahead of the rig move to the next drill location.

Hole AC 21-B

After a ~1.5 miles transit to the north, operations resumed with tagging the seafloor at a driller's depth of 4934 fbrf and spudding Hole AC 21-B at 08h00 on May 4, 2009. Following a protocol designed to maintain good condition at the top of the hole (Collett *et al.*, 2009), the first ~10 ft were drilled with sea water circulation and bit rotation rates of 200 gpm and 10 rpm, respectively. These rates were gradually increased to ~250 gpm and ~50 rpm by 60 fbsf, and maintained until the entire LWD tool string was in the hole (~170 fbsf). At this point, drilling fluid pump flow rate was increased to 350 gpm to activate all the LWD tools, rotation rate was increased to ~90 rpm, and the ROP to ~310 ft/hr. Bit rotation was further increased to ~108 rpm at 220 fbsf.

[1]Borehole Research Group
Lamont-Doherty Earth Observatory
of Columbia University
Palisades, NY 10964
E-mail:
Cook: acook@ldeo.columbia.edu
Guerin: guerin@ldeo.columbia.edu
Mrozewski: stefan@ldeo.columbia.edu

[2]US Geological Survey
Denver Federal Center, MS-939
Box 25046
Denver, CO 80225
E-mail:
tcollett@usgs.gov

[3]National Energy Technology Laboratory
U.S. Department of Energy
P.O. Box 880
Morgantown, WV 26507
E-mail:
ray.boswell@netl.doe.gov

Drilling continued smoothly with sweeps every couple of stands until 285 fbsf when ROP was reduced to ~180 ft/hr. Through the primary target zone, the flow rate was set to the minimum necessary for the LWD tools to run, in order to reduce washouts in the sand-rich sections. All drilling parameters remained generally constant until the total depth of 1116 fbsf was reached at 18h15 on May 4. At 22h00, the well was confirmed static with no apparent flows by the rig's ROV. At 23h30, the decision was made to conclude the project with the AC 21-B hole, and pipe was pulled from the hole and broken down into doubles for offloading.

Data Quality

Hole AC 21-A

Figure F1 displays selected parameters that illustrate the drilling process in Hole AC 21-A and its possible influence on data quality.

The excursions in residual pressure (annulus pressure after subtraction of hydrostatic pressure) and in equivalent circulating density (ECD, a similar measure) observed every ~100 ft are the results of the regular sweeps that were made to clear the hole. No changes in pressure were observed that would have suggested the release of free gas into the borehole or any other potential hazard.

The ROP log, averaged over 5 ft intervals, indicates cyclical spikes that are artifacts due to speed, depth, and/or depth tracking fluctuations occurring immediately before, during and after pipe connections. Most logs are not significantly affected by the high ROP used during the expedition. However, the EcoScope elemental spectroscopy could not be properly calibrated because of the high ROP, and no reliable geochemical logs were recorded.

Ultrasonic and density calipers reveal significant near-seafloor borehole enlargements above ~220 fbsf, responsible for the anomalously low density readings and degraded density image in the shallower ~100 ft (Figures F2 and F3). Below this depth, the hole was in very good condition over most of the section drilled, except for the two main sands (540-555 fbsf and 570-630 fbsf) where both calipers indicate an extremely enlarged hole and suggest that some of the data recorded in these intervals, particularly density and porosity, are unreliable.

EcoScope data, including density measurements, are only acquired after the drilling fluid pump flow rate through the MWD turbine is sufficient to power the tool, which in Hole AC 21-A occurred at 120 fbsf (Figures F2 and F3). When the EcoScope minitron is on, the gamma ray readings of the geoVISION significantly exceed the values measured by the EcoScope because, unlike the EcoScope, it is not compensated for minitron-induced oxygen activation.

The depths relative to seafloor were fixed by identifying the step-like change in the geoVISION gamma ray log at the seafloor. For Hole AC 21-A, the gamma ray log identified the seafloor at 4940 fbrf, in agreement with the initial depth estimated by the drillers. The rig floor logging datum was located 51 ft above sea level.

Hole AC-21-B

Figure F4 displays selected parameters that illustrate the drilling process in Hole AC 21-B and its possible influence on data quality.

The pressure data that were monitored in real-time did not indicate any changes in pressure that would suggest the presence of free gas or any other hazard. The pressure increases observed every ~100 ft are the result of the regular sweeps that were made to help clean the hole.

The ROP log, averaged over 5 ft intervals, indicates cyclical spikes that are artifacts due to speed, depth, and/or depth tracking fluctuations occurring immediately before, during and after pipe connections. Most logs are not significantly affected by the high ROP used during the expedition. However, the EcoScope elemental spectroscopy could not be properly calibrated because of the high ROP, and no reliable geochemical logs were recorded.

The ultrasonic and density calipers logs display significant near-seafloor borehole enlargements above ~140 fbsf, responsible for the anomalously low-density readings and degraded density image in the shallower ~100 ft (Figures F5 and F6). Several spikes and slight enlargements occur on the caliper log between 140 and 520 fbsf, indicating that the density and porosity data measured in these enlarged intervals should be used with caution. Between 520 and 650 fbsf, both calipers indicate an extremely enlarged hole, indicating that some of the data recorded in this sand, particularly density and porosity, are unreliable. The asymmetric Hole Radius image above 650 fbsf in Figure F6

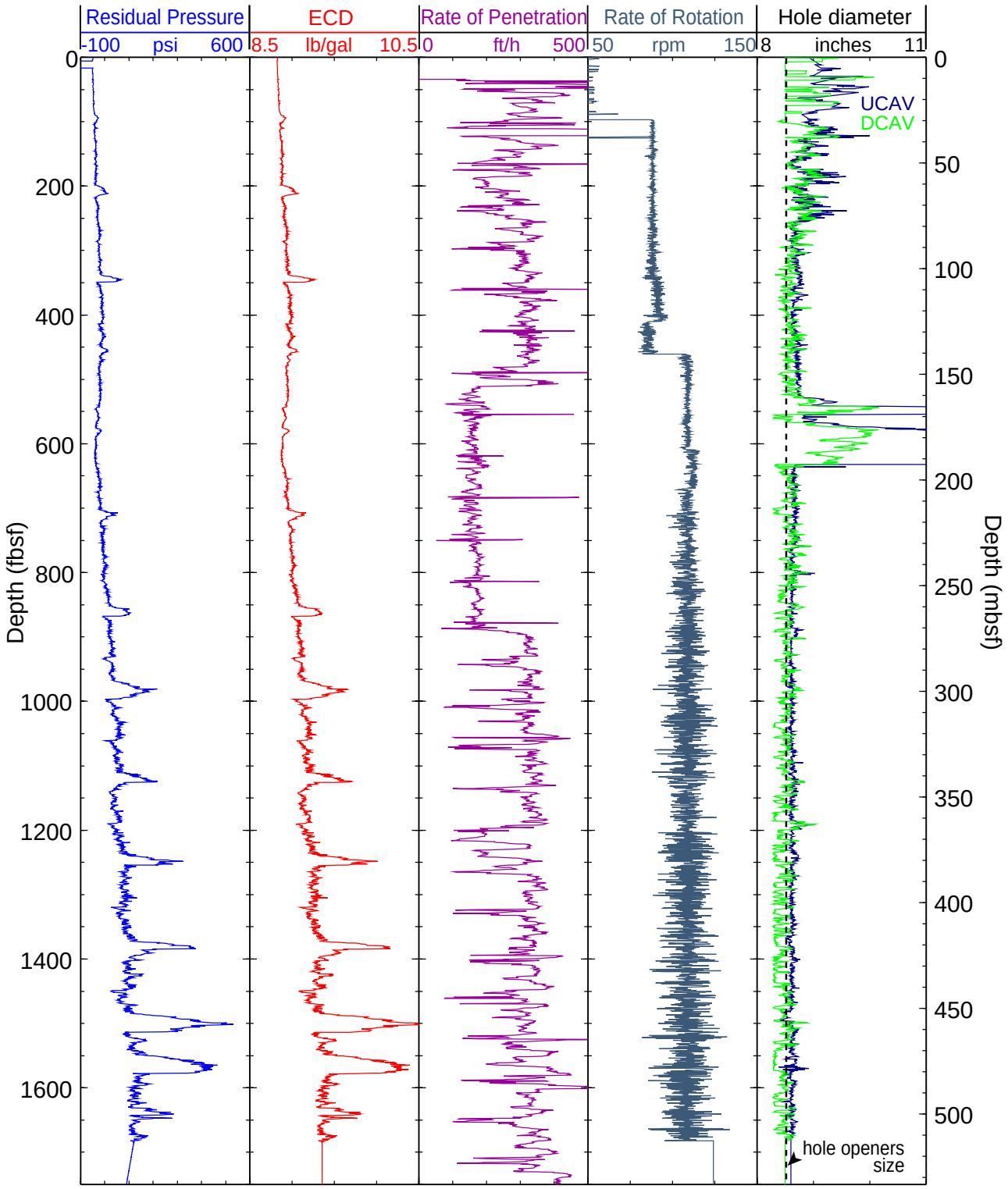

Figure F1: *Monitoring and quality control LWD/MWD logs from Hole AC 21-A. Residual Pressure = Pressure in the annulus after subtraction of the hydrostatic pressure; ECD = Equivalent Circulating Density = effective density of the fluid exerting pressure against the borehole formation; UCAV = Ultrasonic caliper, DCAV = Density caliper.*

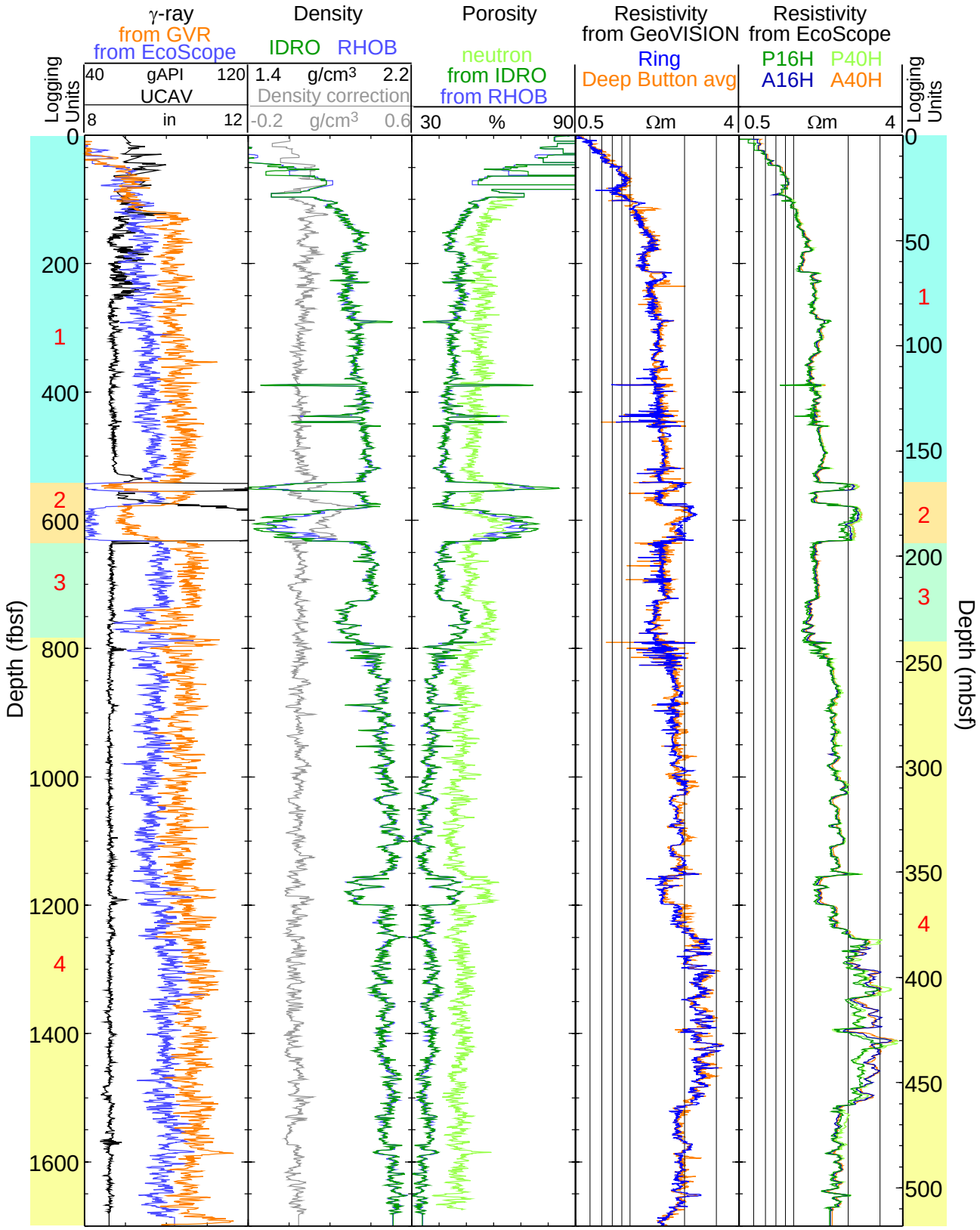

Figure F2: *Summary of LWD log data from Hole AC 21-A. gAPI = American Petroleum Institute gamma ray units, RHOB = Bulk density (EcoScope), IDRO = Image-derived density (EcoScope); neutron = "Best neutron porosity" (EcoScope); Ring = Ring resistivity (geoVISION); PXXH = Phase-shift resistivity at 2 MHz and a transmitter-receiver spacing of XX inches (EcoScope); AXXH = Attenuation resistivity measured at 2 MHz and a transmitter-receiver spacing of XX inches (EcoScope). Logging Units as described in this report are shown.*

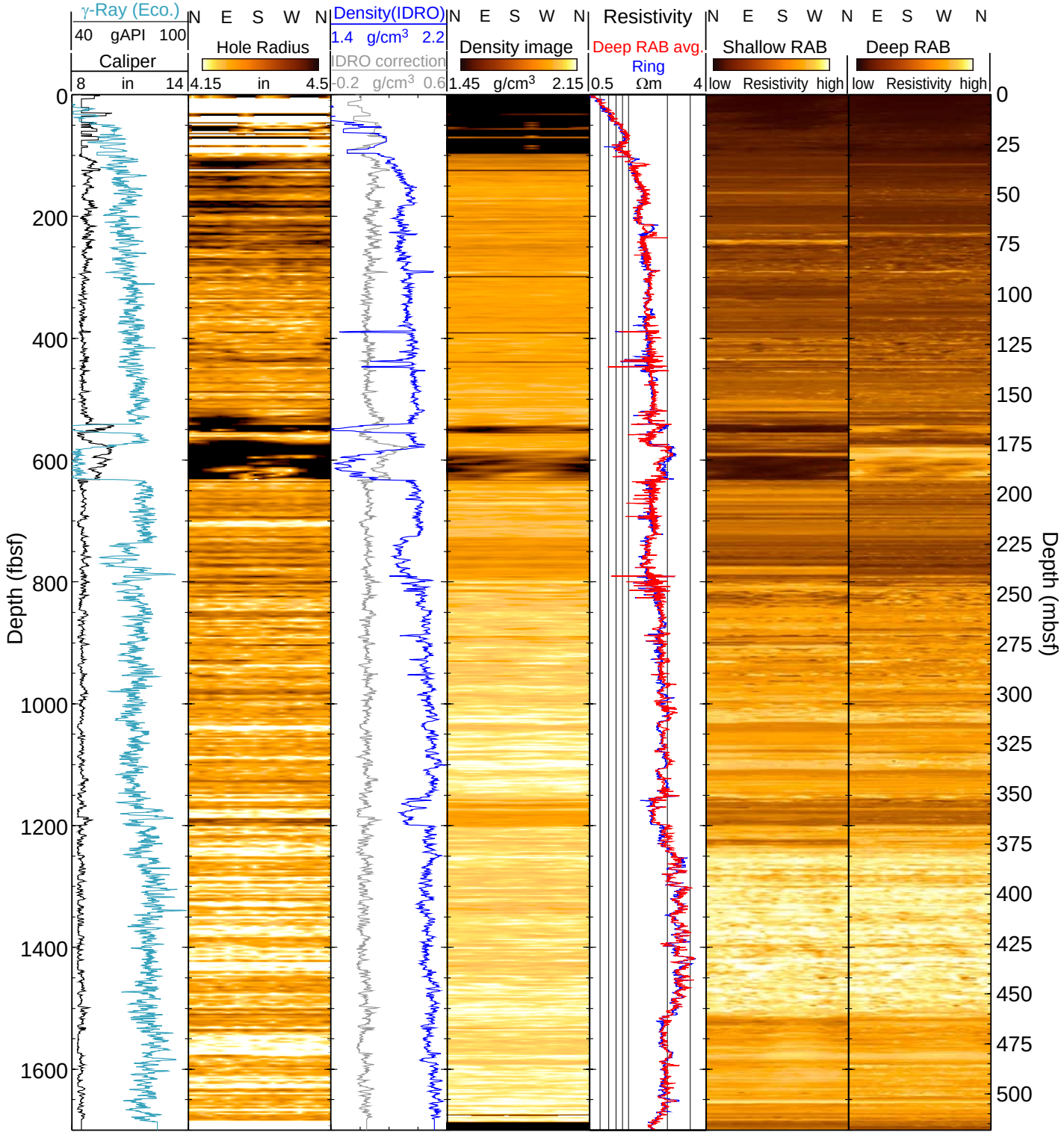

Figure F3: *LWD image data from Hole AC 21-A. gAPI = American Petroleum Institute gamma ray units; RAB = Electrical images obtained by the geoVISION tool; IDRO = Image-derived density (EcoScope). The cardinal directions indicate orientation of the images.*

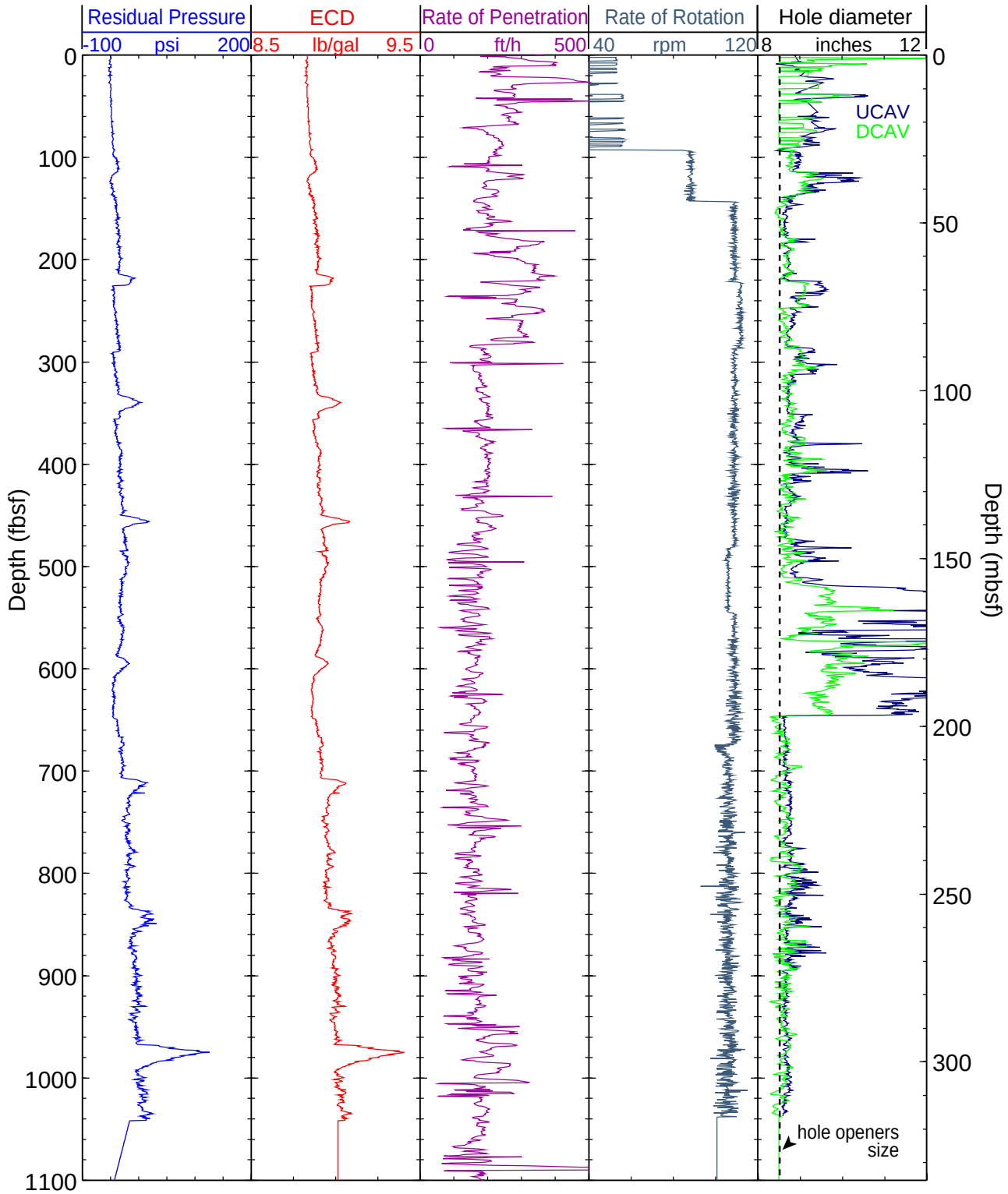

Figure F4: *Monitoring and quality control LWD/MWD logs from Hole AC 21-B. Residual Pressure = Pressure in the annulus after subtraction of the hydrostatic pressure; ECD = Equivalent Circulating Density = effective density of the fluid exerting pressure against the borehole formation; UCAV = Ultrasonic caliper, DCAV = Density caliper.*

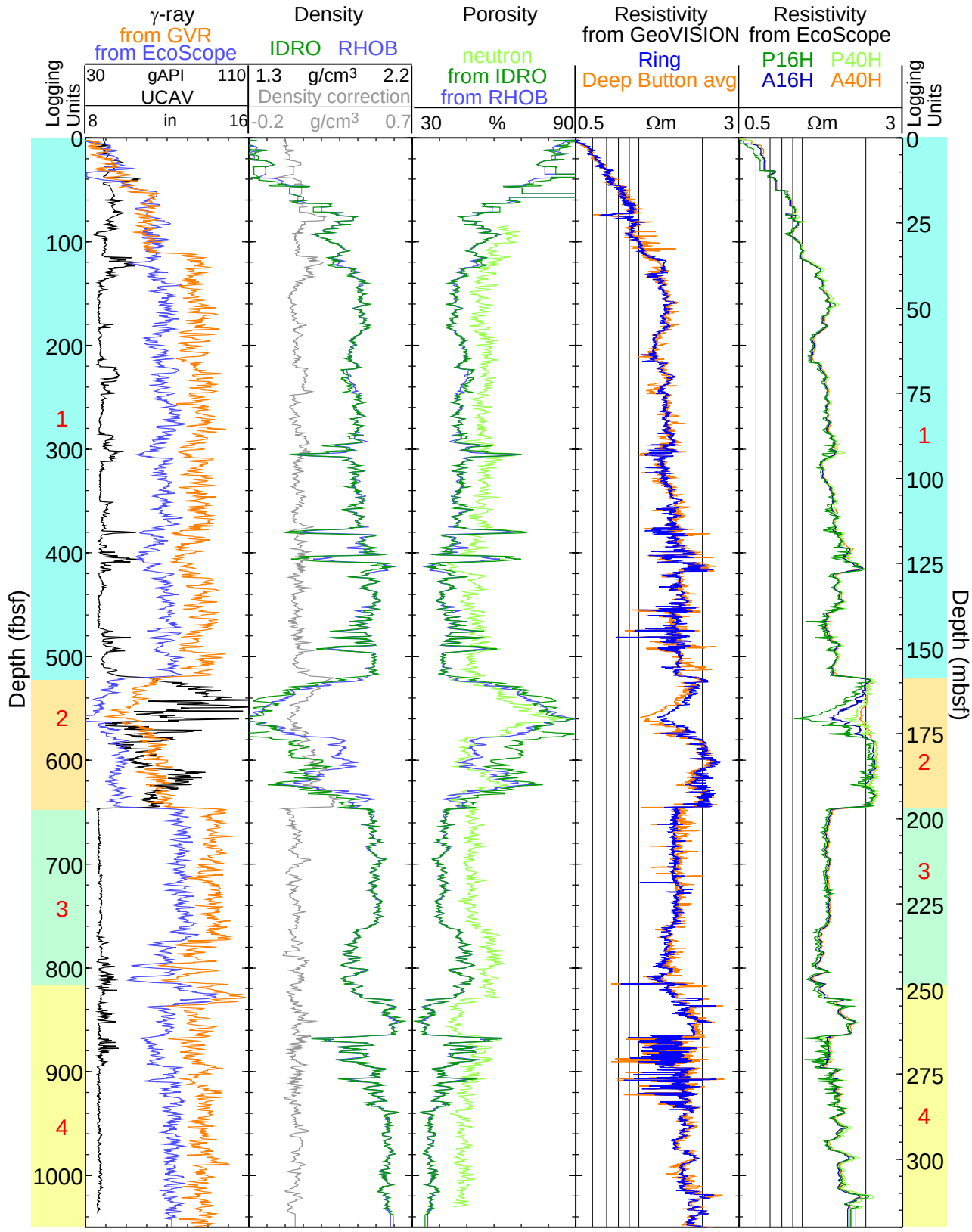

Figure F5: *Summary of LWD log data from Hole AC 21-B. gAPI = American Petroleum Institute gamma ray units, RHOB = Bulk density (EcoScope), IDRO = Image-derived density (EcoScope); neutron = "Best neutron porosity" (EcoScope); Ring = Ring resistivity (geoVISION); PXXH = Phase-shift resistivity at 2 MHz and a transmitter-receiver spacing of XX inches (EcoScope); AXXH = Attenuation resistivity measured at 2 MHz and a transmitter-receiver spacing of XX inches (EcoScope). Logging Units as described in this report are shown.*

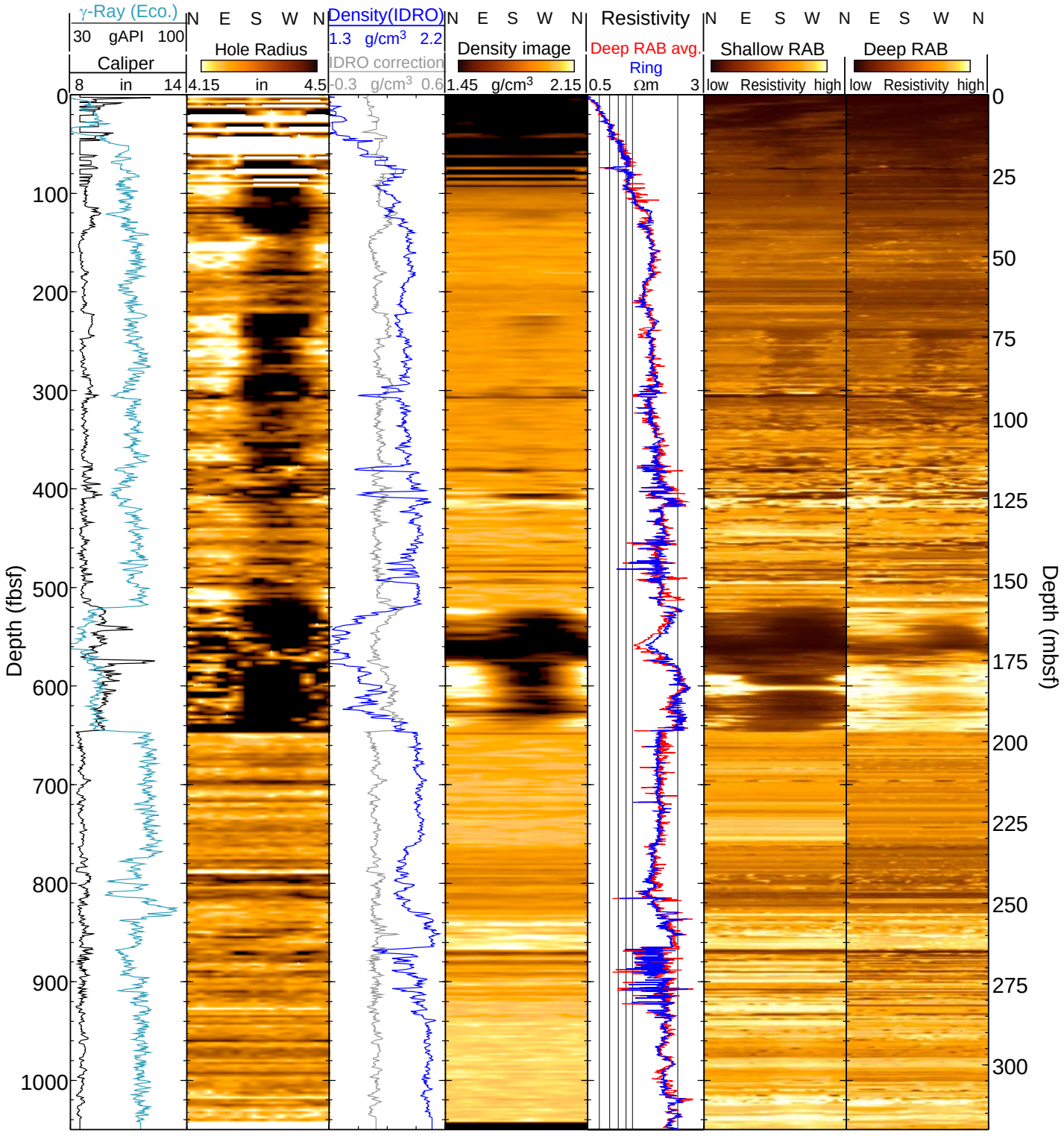

Figure F6: *LWD image data from Hole AC 21-B. gAPI = American Petroleum Institute gamma ray units; RAB = Electrical images obtained by the geoVISION tool; IDRO = Image-derived density (EcoScope). The cardinal directions indicate orientation of the images.*

suggests either that the hole was asymmetrical, or that the tool string was leaning on the eastern side of the borehole because of the slight western deviation of the hole. The shallow geoVISION images in Figure F3 were also affected by the enlarged hole conditions in the target sand. Below 650 fbsf, the hole was mostly in gauge and all data should be of good quality.

EcoScope data are only acquired once flow through the MWD turbines is sufficient to power the tool, which in AC 21-B occurred at ~110 fbsf for gamma ray measurements (Figures F5 and F6). Once the EcoScope minitron is on, the gamma ray readings of the geoVISION significantly exceed the values measured by the EcoScope because, unlike the EcoScope, it is not compensated for minitron-induced oxygen activation.

The depths relative to seafloor were fixed by identifying the step change in the geoVISION gamma ray log at the seafloor. For Hole AC 21-B, the gamma ray log identified the seafloor at 4934 fbrf, in agreement with the initial depth estimated by the drillers. The rig floor logging datum was located 51 ft above sea level.

Interpretation of LWD Logs

Logging Displays Overview

The combined analysis of the different logs and images recorded by the LWD tools in Holes AC 21-A and AC 21-B delineates several logging units with distinct trends and features that can be observed in the two holes drilled in the Alaminos Canyon Block 21 area and correlated to the seismic stratigraphy as described in detail by Frye *et al.* (2009) in the Alaminos Canyon 21 Site Summary. Logging units are defined primarily by the character of the logs. They are usually, but not necessarily, related to geological, seismic or other interpretations.

Figures F2 and F5 show the main logs recorded by the geoVISION and the EcoScope tools in Holes AC 21-A, and AC 21-B, respectively. As noted in the ***Data Quality*** section, the offset between the gamma ray logs recorded by the two tools is the result of neutron activation in the formation by the EcoScope minitron source on the readings of the geoVISION tool. Despite this offset, the two tools display identical trends, and only the EcoScope gamma ray is used in the following discussion.

Figures F3 and F6 give a summary of some of the images recorded by the geoVISION and EcoScope tools. While showing the same measurements as the log curves, and allowing the same type of correlations, the azimuthal images illustrate the influence of structure and heterogeneity on the isotropic measurements captured by the logs.

Figures F7 and F8 display the compressional velocity data recorded by the MP3 and the sonicVISION tools. In addition to the V_p logs, the monopole waveforms and the slowness-time coherence (STC) projections used to derive V_p provide an assessment of the quality of the acoustic data and of the attenuating effect of gas hydrate. All V_p logs were refined by post cruise processing and can be reliably used for seismic correlation.

In each of these figures, the gamma ray and resistivity curves provide a common indication of the variations in lithology and/or gas hydrate occurrence.

Logging Units

The sequence drilled in the two holes in the Diana sub-basin contains elements of submarine fan deposition within a Gulf of Mexico slope mini-basin (Frye *et al.*, 2009). Because Hole AC 21-A penetrated deeper in the sequence than Hole AC 21-B, the interpretation is mostly based on the data recorded in this hole. The four logging units identified are primarily defined by trends in the resistivity, sonic and gamma ray logs that were less affected by the degraded borehole conditions than other logs.

Logging Unit 1 extends from the surface to 541 fbsf in Hole AC 21-A, and to 520 fbsf in Hole AC 21-B. It is characterized by a steady increase downward in gamma ray, density, resistivity and sonic velocity.

Logging Unit 2 is represented in both holes by the target sands (541 to 633 fbsf in Hole AC 21-A; 520 to 648 fbsf in Hole AC 21-B). It coincides also with the interval where borehole conditions were the most degraded, which makes it difficult to assess its characteristics with confidence. Slightly higher resistivity values than in the adjacent sections suggest some accumulation of gas hydrate, which is confirmed by the higher velocity measured by the MP3 tool, particularly in the deeper sand in Hole AC 21-B (Figures F7 and F8). The absence of similar velocity values in the data recorded by the SonicVISION tool might be partially due to the location of this tool higher in the tool string, but it is not yet fully

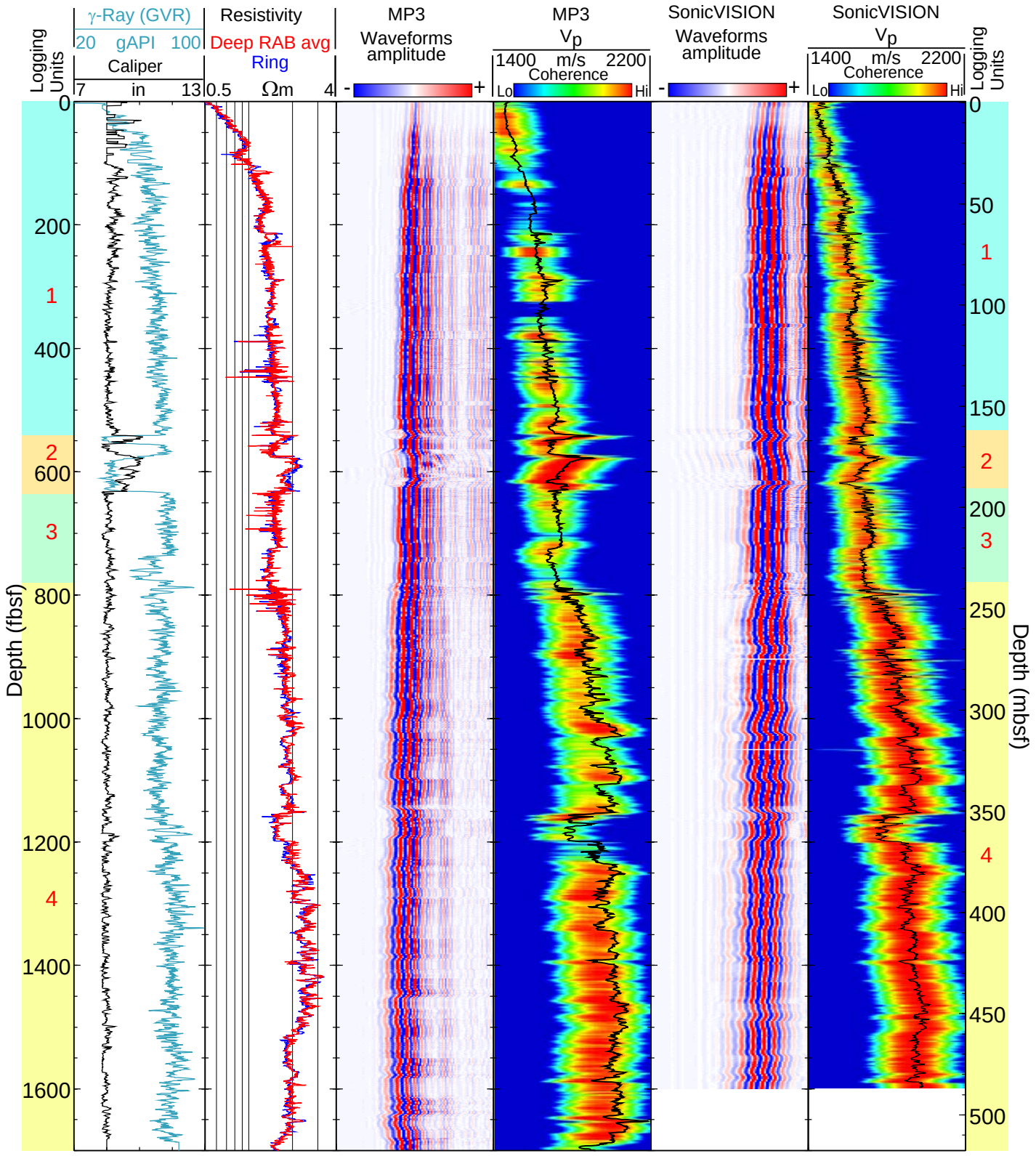

Figure F7: *Sonic waveform data and P-wave velocities recorded by the MP3 and sonicVISION tools in Hole AC 21-A. Coherence projections resulting from the slowness-time coherence processing give an indication of the quality and reliability of the data. V_p = P-wave velocity. Logging Units as described in this report are shown.*

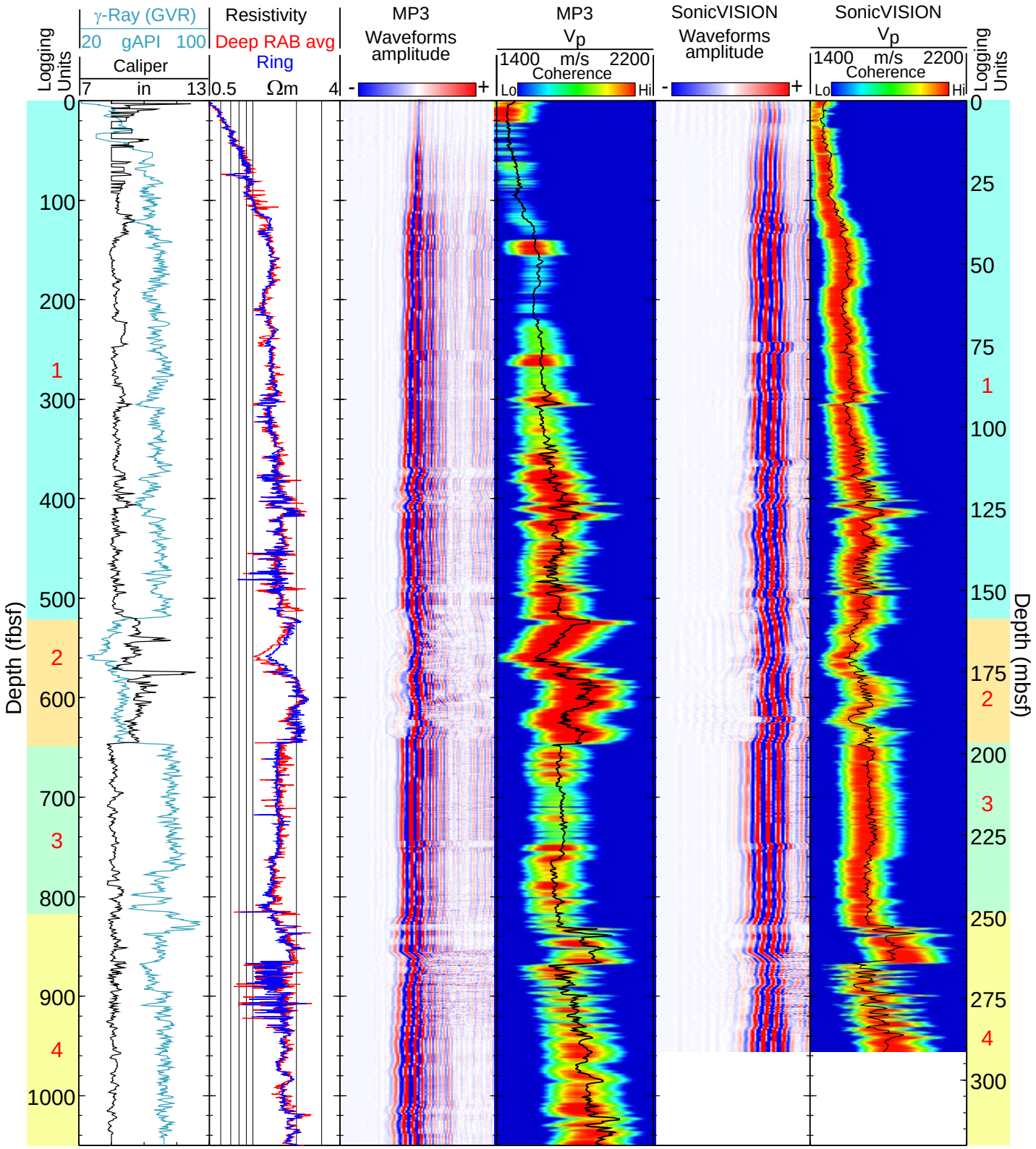

Figure F8: *Sonic waveform data and P-wave velocities recorded by the MP3 and sonicVISION tools in Hole AC 21-B. Coherence projections resulting from the slowness-time coherence processing give an indication of the quality and reliability of the data. V_p = P-wave velocity. Logging Units as described in this report are shown.*

explained, and suggests that any gas hydrate accumulation should be relatively minor (see ***Gas Hydrate and Free Gas Occurrence***).

Logging Unit 3 is made of a ~150 ft thick clay-rich section and of a sandy interval indicated by lower gamma ray readings (Figures F2 and F5), separated by an abrupt decrease in density, resistivity and velocity (at ~740 fbsf in Hole AC 21-A and ~770 fbsf in Hole AC 21-B). It coincides mostly with the sequence of sub-horizontal reflectors overlying the Regional 1 seismic horizon (Frye *et al.*, 2009).

The increase in resistivity, velocity and density that define the top of Logging Unit 4 (at ~780 fbsf in Hole AC 21-A and ~820 fbsf in Hole AC 21-B) are likely responsible for the Regional 1 horizon, which defines a major depositional boundary (Frye *et al.*, 2009). Velocity, resistivity and density increase steadily with depth throughout Logging Unit 4. This unit extends to the bottom of each hole, but the general trend of the depositional sequence is mainly apparent in Hole AC 21-A because of its deeper penetration. Resistivity values slightly above the apparent baseline in clay sediments between ~1250 and 1500 fbsf in Hole AC 21-A may or may not be related to gas hydrate-filled fractures (see ***Gas Hydrate and Free Gas Occurrence***).

LWD Borehole Images

The geoVISION and EcoScope tools generate high-resolution images of borehole log data. The EcoScope tool produces images of density and hole radius (computed on the basis of the density correction, which is a function of borehole standoff), as well as gamma ray and photoelectric factor. The geoVISION produces a gamma ray image and shallow, medium and deep depth of investigation resistivity images.

Figures F3 and F6 show some of the LWD images collected by the EcoScope and geoVISION tools in Holes AC 21-A and AC 21-B. The unwrapped images are about 70 cm wide (for an 8.75 inch diameter borehole) and the vertical scale is highly compressed relative to the horizontal.

In both holes, the most prominent features are the target sands (541-556 and 571-633 fbsf in Hole AC 21-A; 520 to 650 fbsf in AC 21-B) where the hole radius is enlarged and the density and shallow resistivity images are clearly affected by the bad hole condition. The deep button image is acquired deep enough into the formation to illustrate higher formation resistivity and the possible presence of gas hydrate. In addition, the resistivity image in Figure F3 displays a mottled, higher resistivity section from 1250 to 1515 fbsf, which correlates with an inferred mass transport complex on the seismic sections (Frye *et al.*, 2009).

Gas Hydrate and Free Gas Occurrence

The target sands in the Alaminos Canyon sites, (541-556 fbsf and 571-633 fbsf in Hole AC 21-A, 520-648 fbsf in Hole AC 21-B) display slightly higher resistivity values, near 2 Ω-m, than the ~1.5 Ω-m baseline in the surrounding clays. The compressional velocity measured by the MP3 tool also indicates higher readings in the target sands, particularly in the lower section of the AC 21-B target (Figure F8), combining with the increased resistivity to suggest that some amount of gas hydrate may be present. However, the velocity measured by the sonicVISION tool does not display any matching increase (Figures F7 and F8). It is possible that some of the gas hydrate detected by the MP3 tool had dissociated by the time the sonicVISION tool reached the sand unit. Thus, any accumulation of gas hydrate should be minimal. Other factors that may contribute to the resistivity response seen in the sands may be lower pore water salinity, lower porosity, or resistive mineralized deposits in the sands. Further data collection will be necessary to enable more confident interpretation. Even though, we applied resistivity-based gas hydrate saturation estimation techniques in the event that the slightly higher resistivity values measured in Holes AC 21-A and AC 21-B were due to natural gas hydrate.

In Hole AC 21-A, the target sands are made of two intervals: a 15 ft interval from 541 to 556 fbsf, and a ~62 ft sand from 571 to 633 fbsf (Figure F9). In Hole AC 21-B, the target sand is one 128-foot interval from 520 to 648 fbsf (Figures F10 and F11). The caliper in both holes indicates an extremely enlarged borehole in the target sands. The enlarged hole significantly affects the density and neutron porosity measurements, producing lower than expected porosity values. In addition, because of the narrow resistivity range measured, the selection of the Archie cementation exponent m and the identification of the water-saturated formation resistivity R_o significantly affects the calculated hydrate saturations. Consequently, we used two methods to estimate gas hydrate saturations in the Alaminos Canyon wells: Archie's standard method and Archie's quick look approach. These techniques are described in Mrozewski *et al*. (2009).

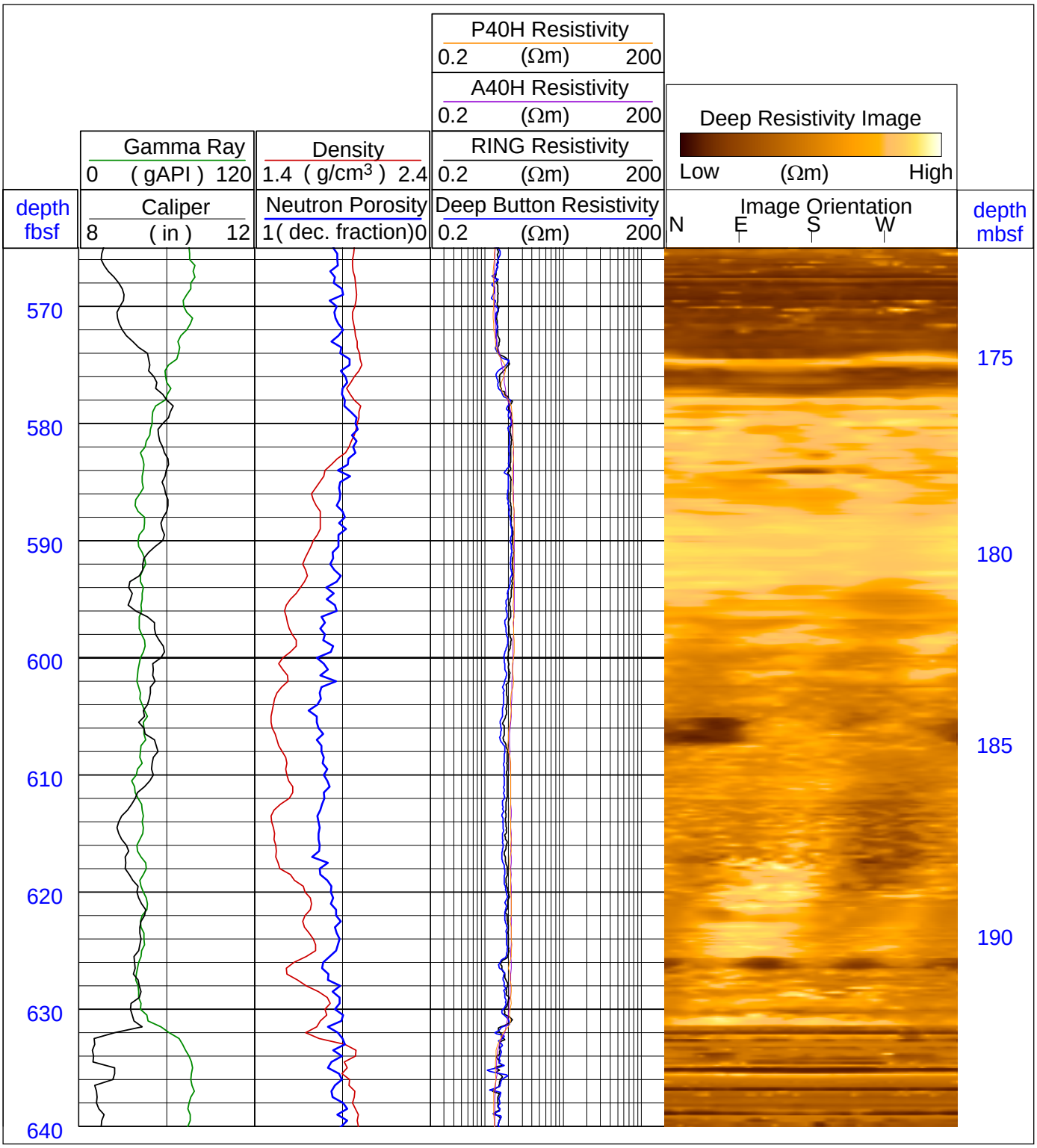

Figure F9: *Logs and LWD resistivity image from 565 to 640 fbsf in Hole AC 21-A, showing the target sand unit in this hole. Ring = Ring resistivity (geoVISION); P40H = Phase-shift resistivity at 2 MHz and a transmitter-receiver spacing of 40 inches (EcoScope); A40H = Attenuation resistivity measured at 2 MHz and a transmitter-receiver spacing of 40 inches (EcoScope).*

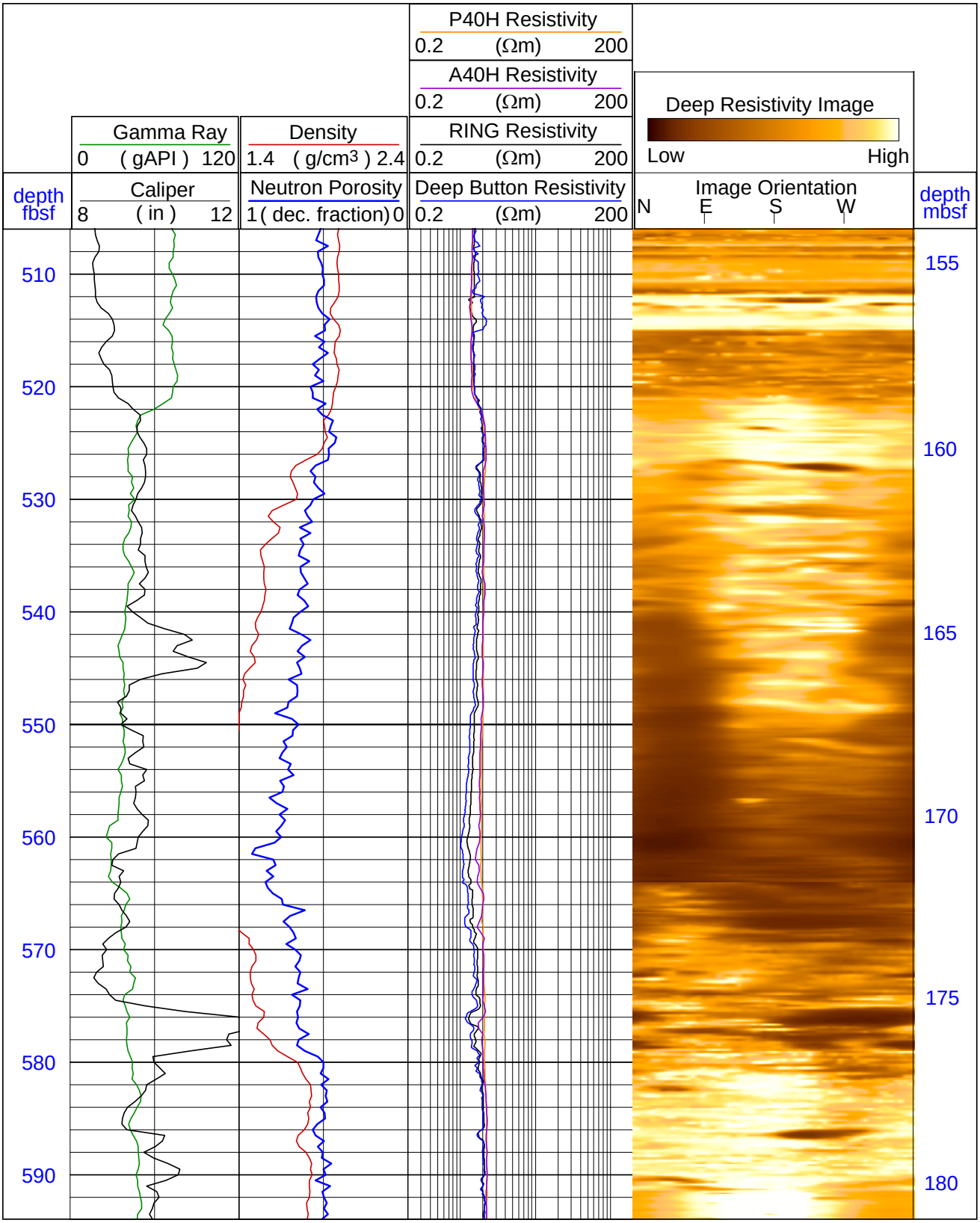

Figure F10: *Logs and LWD resistivity image from 506 to 594 fbsf in Hole AC 21-B showing the top section of the target sand unit. Ring = Ring resistivity (geoVISION); P40H = Phase-shift resistivity at 2 MHz and a transmitter-receiver spacing of 40 inches (EcoScope); A40H = Attenuation resistivity measured at 2 MHz and a transmitter-receiver spacing of 40 inches (EcoScope).*

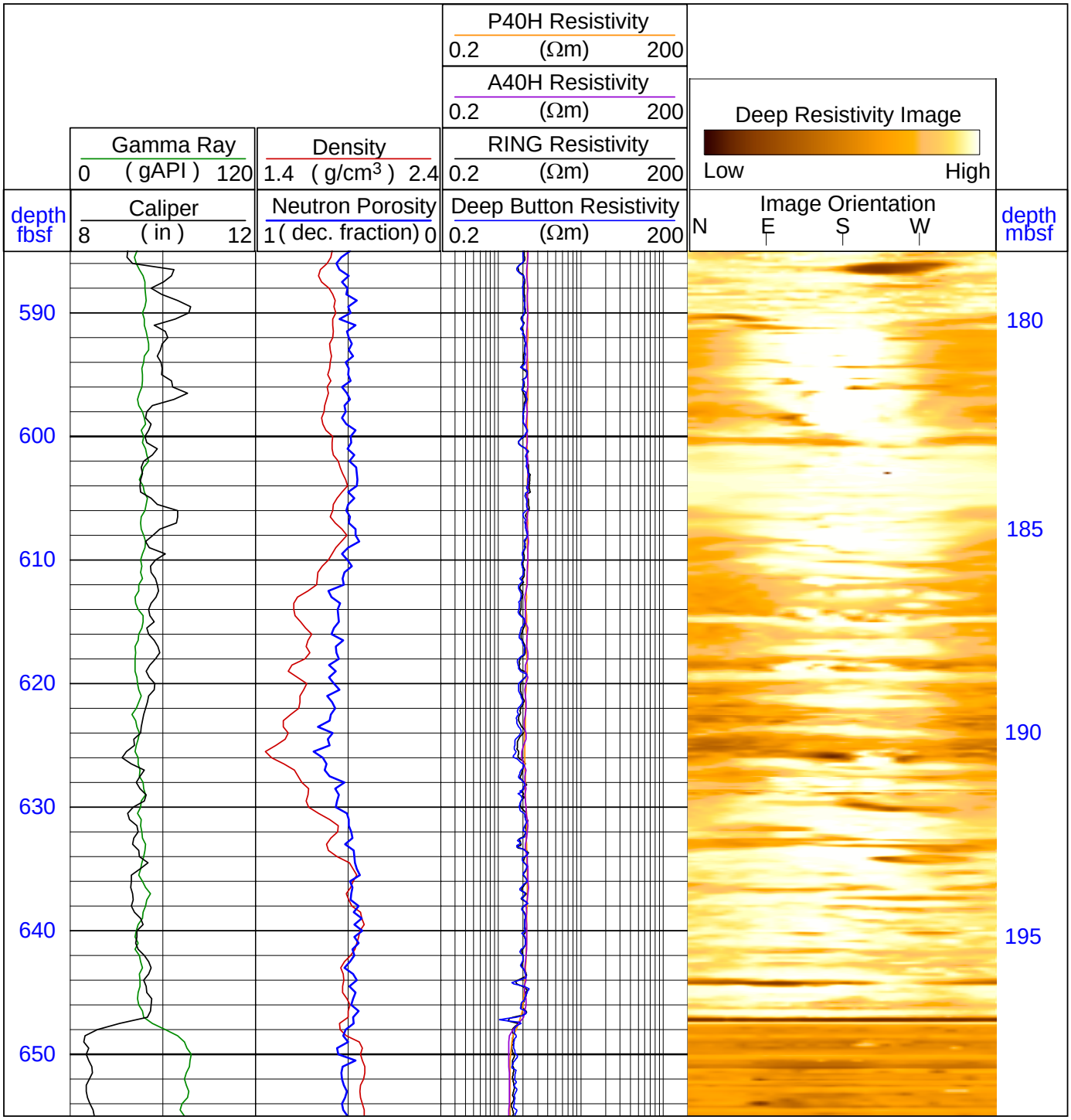

Figure F11: *Logs and LWD resistivity image from 585 to 655 fbsf in Hole AC 21-B, showing the basal section of the target sand unit. Ring = Ring resistivity (geoVISION); P40H = Phase-shift resistivity at 2 MHz and a transmitter-receiver spacing of 40 inches (EcoScope); A40H = Attenuation resistivity measured at 2 MHz and a transmitter-receiver spacing of 40 inches (EcoScope).*

The gamma ray values in the sands in both Holes AC 21-A and AC 21-B range from 40 to 45 API, much lower than the surrounding clay-rich sediments, which exhibit gamma ray values of 70-80 API. A relatively thin stratigraphic section with slightly lower gamma ray value of ~65 API, occurs about 100 ft below the target sands, between 737 and 774 fbsf in Hole AC 21-A and between 778 and 815 fbsf in Hole AC 21-B. In these sandier intervals, the value of the cementation exponent m providing the best fit for the water-saturated resistivity R_o is m = 2.3. The calibration intervals, however, are not nearly as clean as the target sands and may not be indicative of the correct cementation exponent in the target sands. In the clay intervals, a value of m = 2 was applied. Depending on the value of the chosen saturation exponent (n), the highest gas hydrate saturations in Holes AC 21-A and AC 21-B are 30% or 50% (Figures F12 and F13).

Because of the significant borehole enlargements in the sand intervals in both holes, and because of the extremely high porosity values measured, Archie's quick look likely provides a more accurate estimation of gas hydrate saturation in the Alaminos Canyon sites. For this method, two different baseline resistivity (R_o) values were chosen. A conservative value of R_o = 1.5 Ω-m reflects the resistivity of the clay sediments surrounding the target sands. A baseline value more favorable for gas hydrate occurrence is R_o = 0.9 Ω-m, which is the lowest measured resistivity in the relatively clay-rich sections from 737 to 774 fbsf in Hole AC 21-A and from 778 to 815 fbsf in Hole AC 21-B (Figures F14, F15, F16 and F17). The higher R_o baseline of 1.5 Ω-m produces lower hydrate saturations between 0-20%. When the baseline is assumed to be 0.9 Ω-m, gas hydrate saturations are higher with maximum values between 30%-50%.

Aside from the target sands, Hole AC 21-A also displays a slightly higher resistivity section between 1250 and 1515 fbsf. The top of this interval (Figure F18) correlates with the top of a mass transport complex (MTC) interpreted from the seismic sections (Frye *et al.*, 2009), but the base of the MTC is deeper than 1515 fbsf. Archie's equation suggests that gas hydrate could fill 20 to 30 % of the pore space between 1250 and 1515 fbsf. However, the sonicVISION shows no appreciable increase in compressional velocity, suggesting that little or no gas hydrate is present in this interval. Some very small separations between long spacing (A40H, P40H) and short spacing (A16H, P16H) propagation resistivity in this interval may indicate gas hydrate-filled fractures. The resistivity images do display a few resistive partial sinusoidal features in this interval, but they do not look similar to gas hydrate-filled fractures seen in Green Canyon block 955 (Guerin *et al*., 2009), Walker Ridge block 313 (Cook *et al.*, 2009) or in the JIP 1 Keathley Canyon block 151 holes (Cook *et al.*, 2008). For example, the images from 1250-1515 fbsf in Hole AC 21-A lack the resistive halo seen usually at the peak and trough of gas hydrate-filled fracture.

Conclusion

Because of the bad hole conditions in the target sands in the Alaminos Canyon 21 wells, the characterization of the gas hydrate accumulation in this turbidite channel/ lobe complex is not as complete as in the other sites drilled during the JIP Leg II LWD program. However, a few conclusions can be drawn:

- The acoustic and resistivity logs indicate that some gas hydrate may be present in the target sands.
- Gas hydrate saturation is estimated to be at most 50% in some part of the target sands, but more likely less than 30%.
- Some gas hydrate might also be present deeper in the section in Hole AC 21-A, in the clay-rich interval from 1250 to 1515 fbsf.

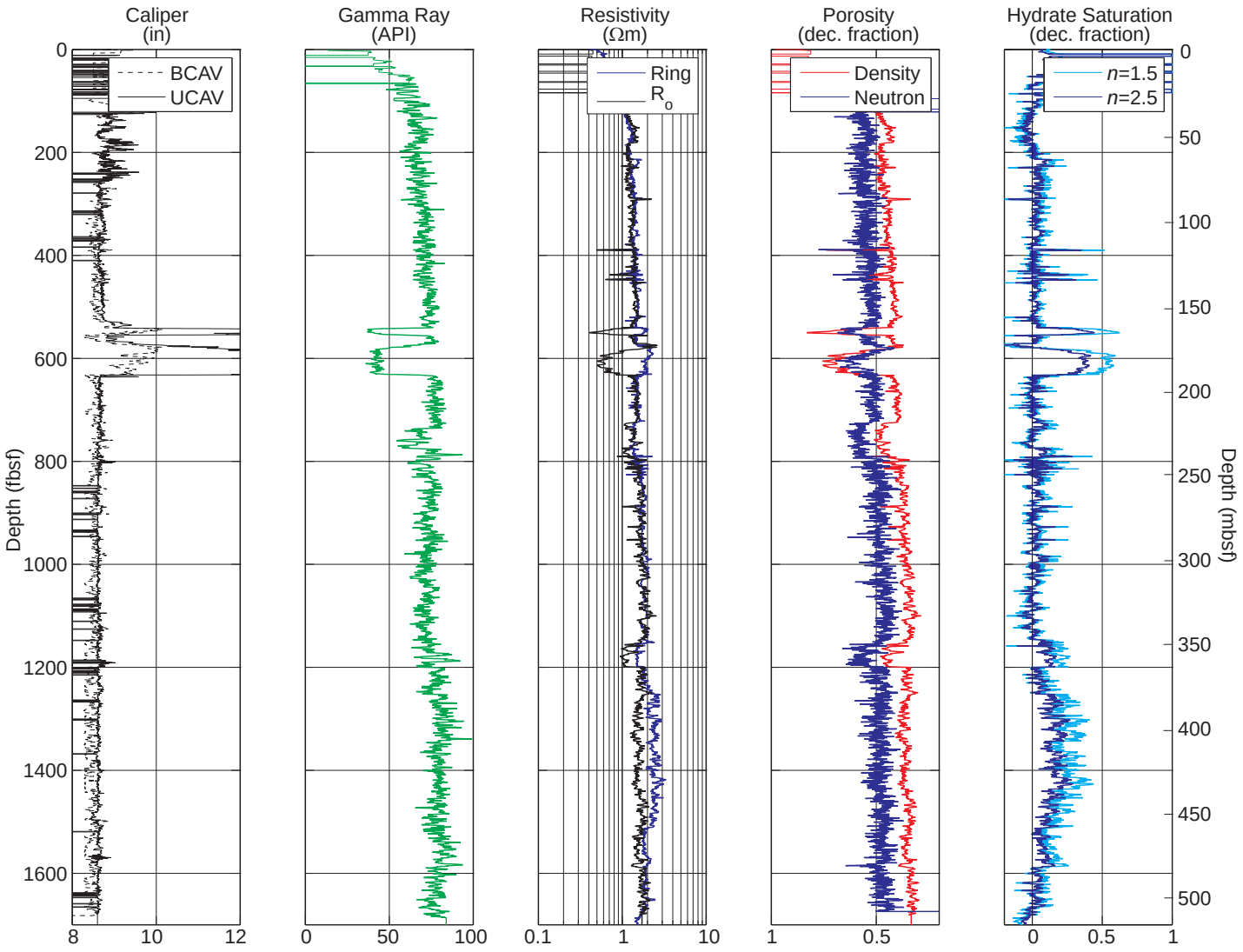

Figure F12: *Results of Archie's equation applied to the porosity and resistivity logs in Hole AC 21-A. R_0 = Computed formation resistivity for 100% water saturation.*

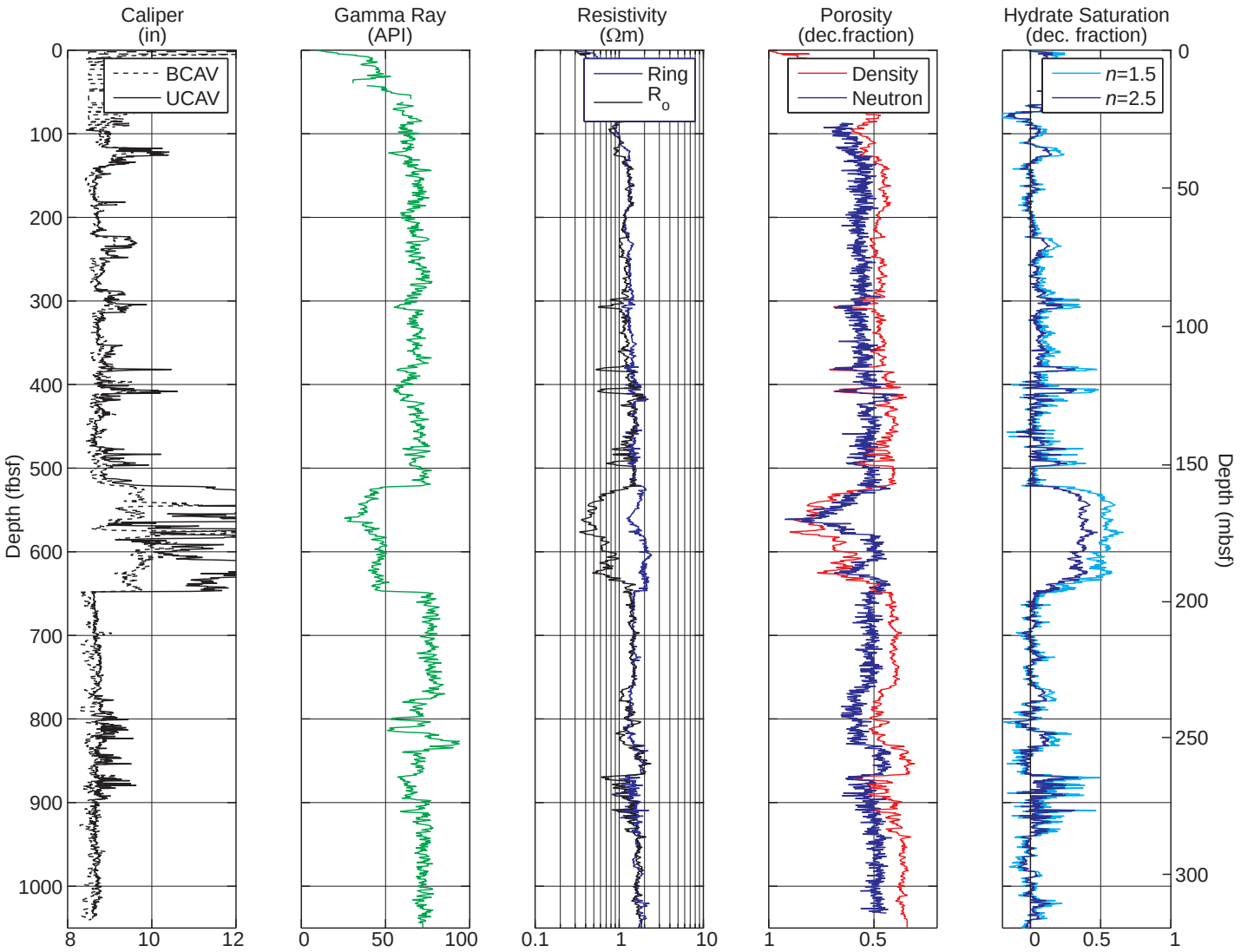

Figure F13: *Results of Archie's equation applied to the porosity and resistivity logs in Hole AC 21-B. R_0 = Computed formation resistivity for 100% water saturation.*

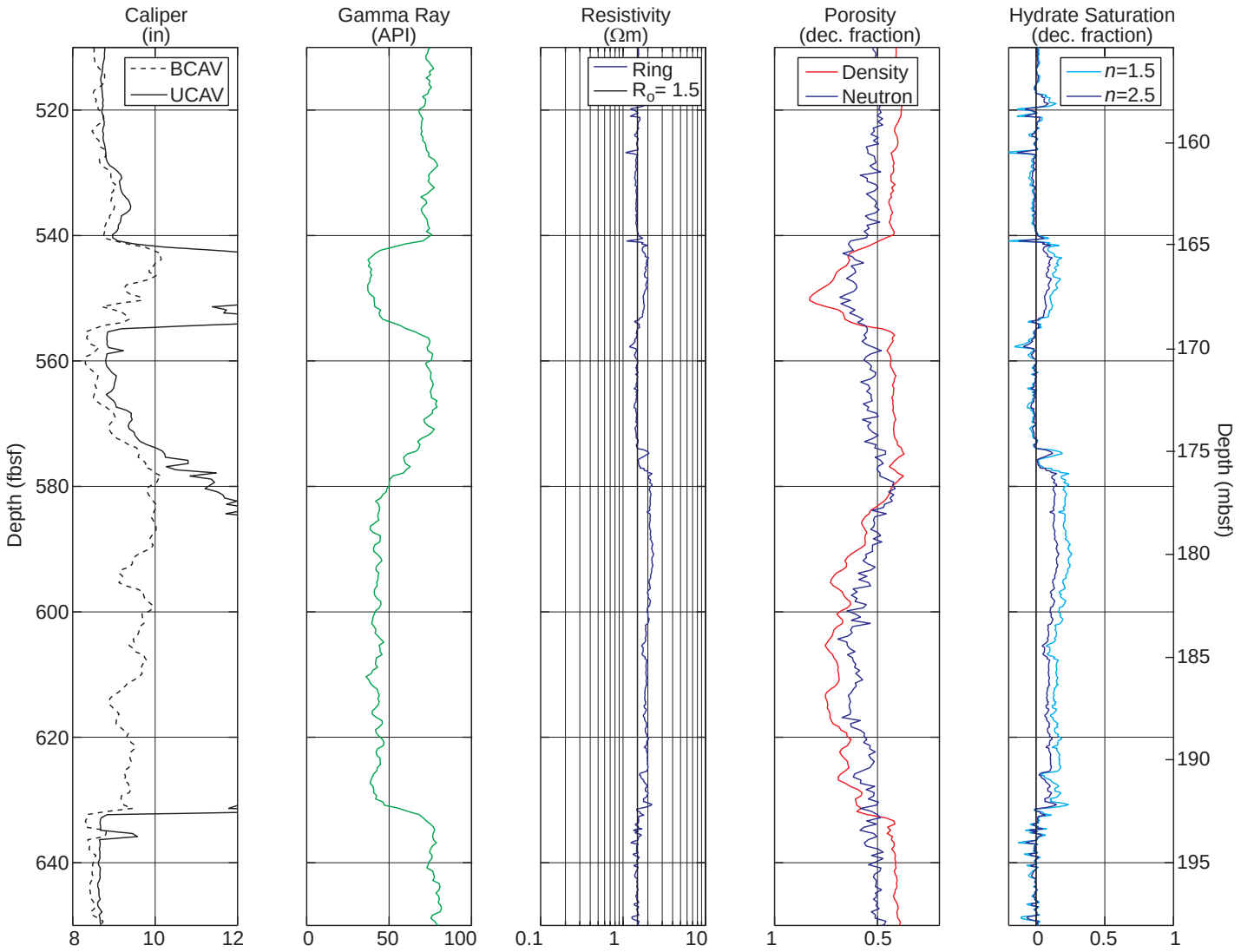

Figure F14: *Results of Archie's quick look technique applied to the porosity and resistivity logs in Hole AC 21-A for the target sand interval with the baseline R_0 = 1.5 Ω-m.*

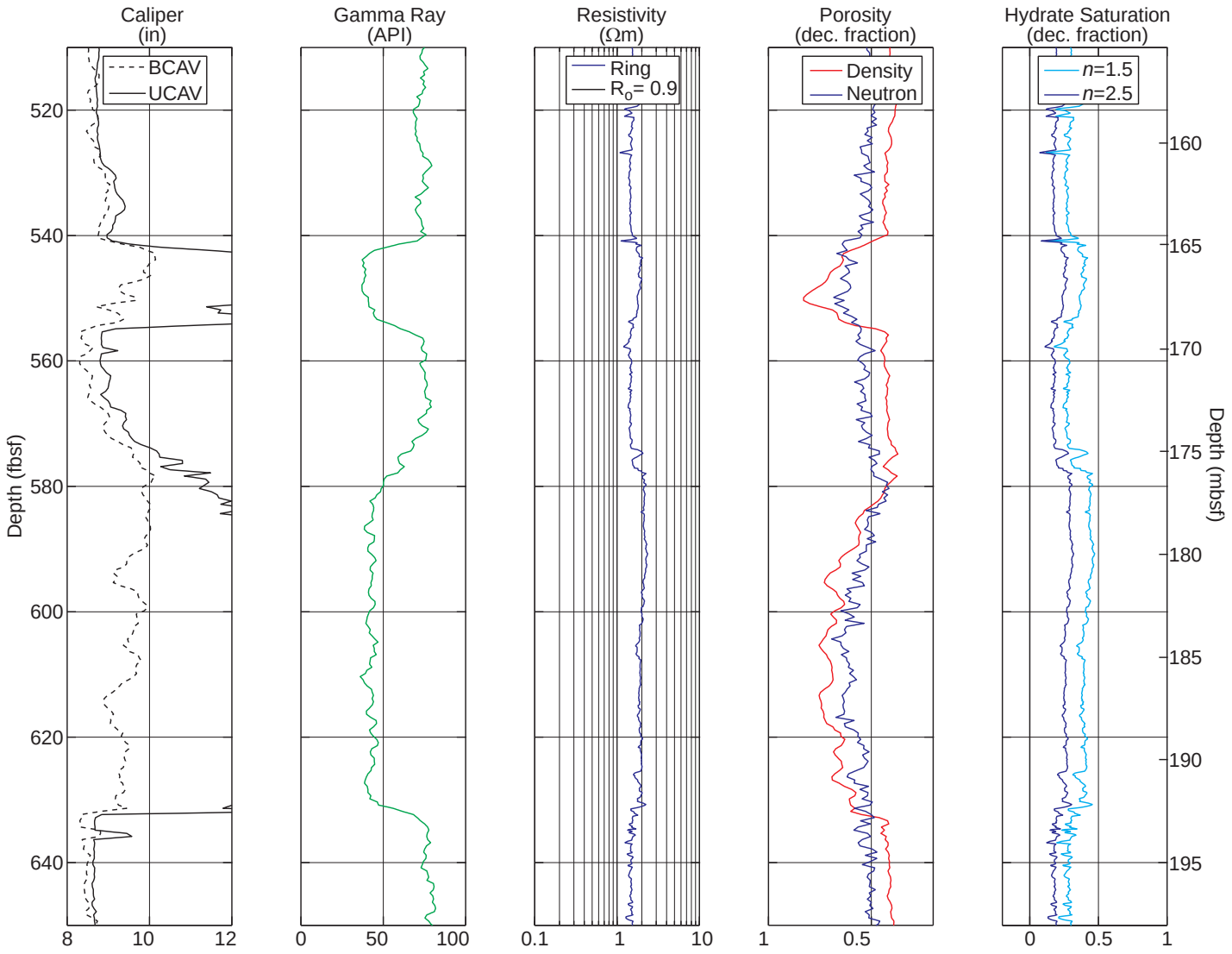

Figure F15: *Results of Archie's quick look technique applied to the porosity and resistivity logs in Hole AC 21-A for the target sand interval with the baseline R_0 = 0.9 Ω-m.*

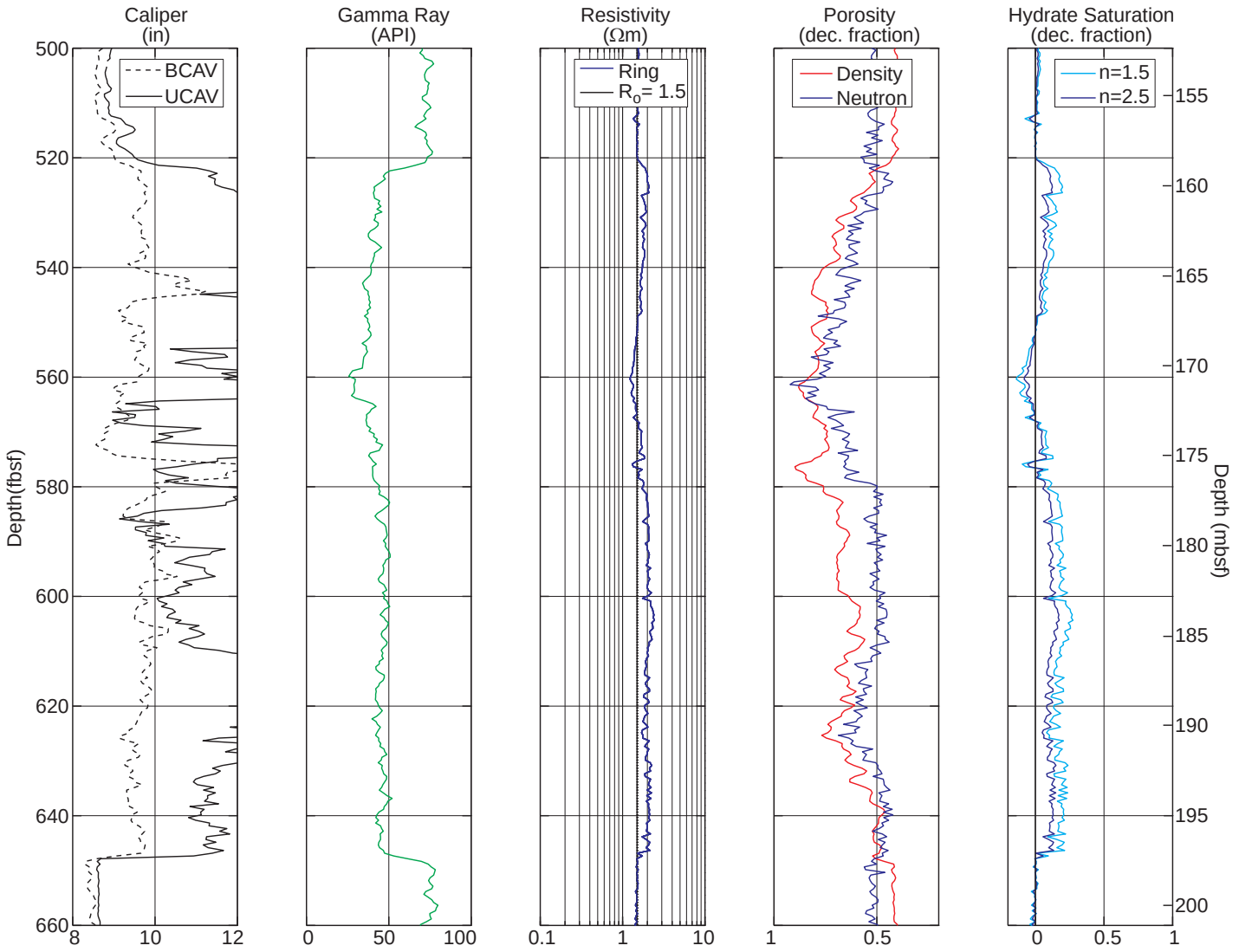

Figure F16: *Results of Archie's quick look technique applied to the porosity and resistivity logs in Hole AC 21-B for the target sand interval with the baseline R_0 = 1.5 Ω-m.*

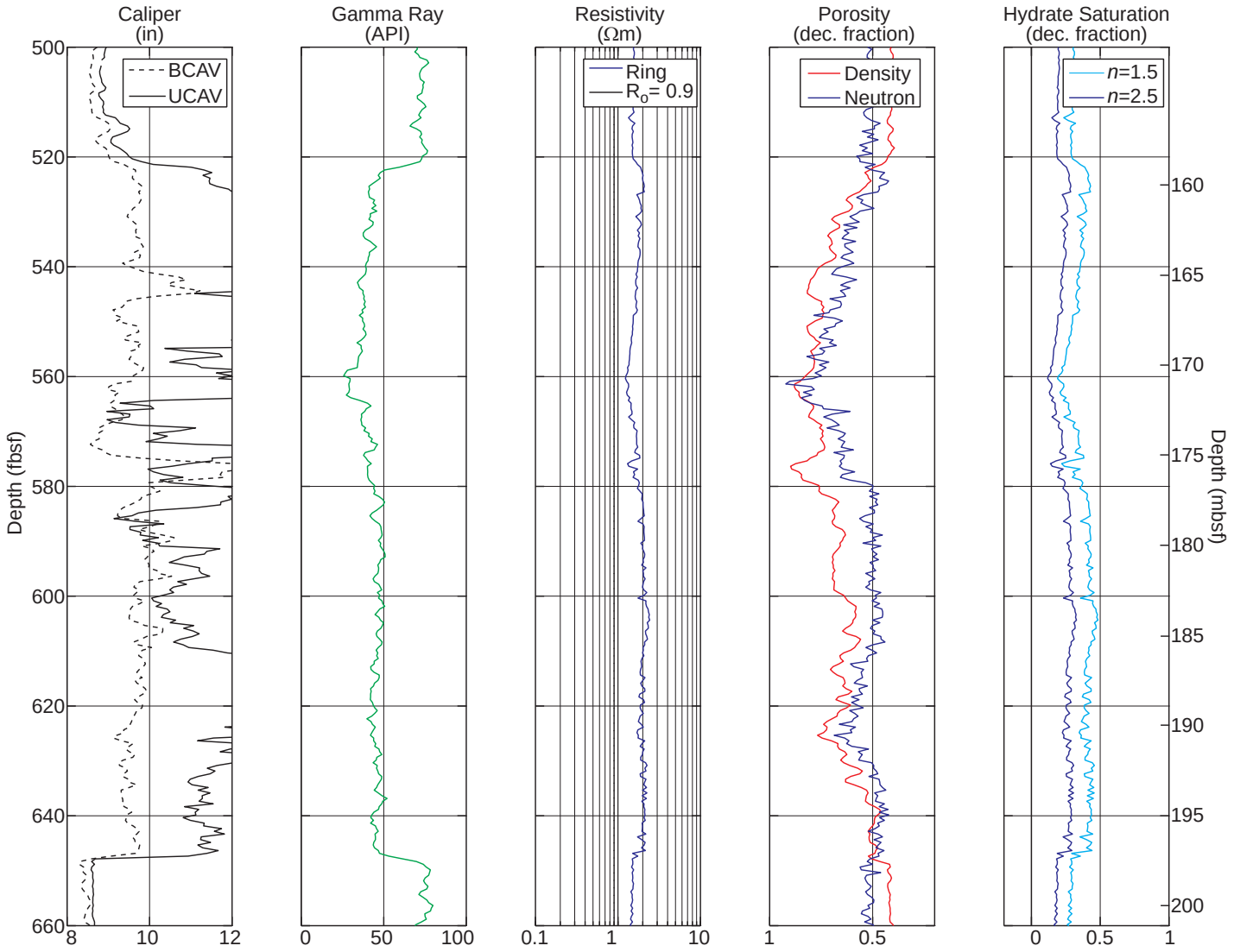

Figure F17: *Results of Archie's quick look technique applied to the porosity and resistivity logs in Hole AC 21-B for the target sand interval with the baseline R_0 = 0.9 Ω-m.*

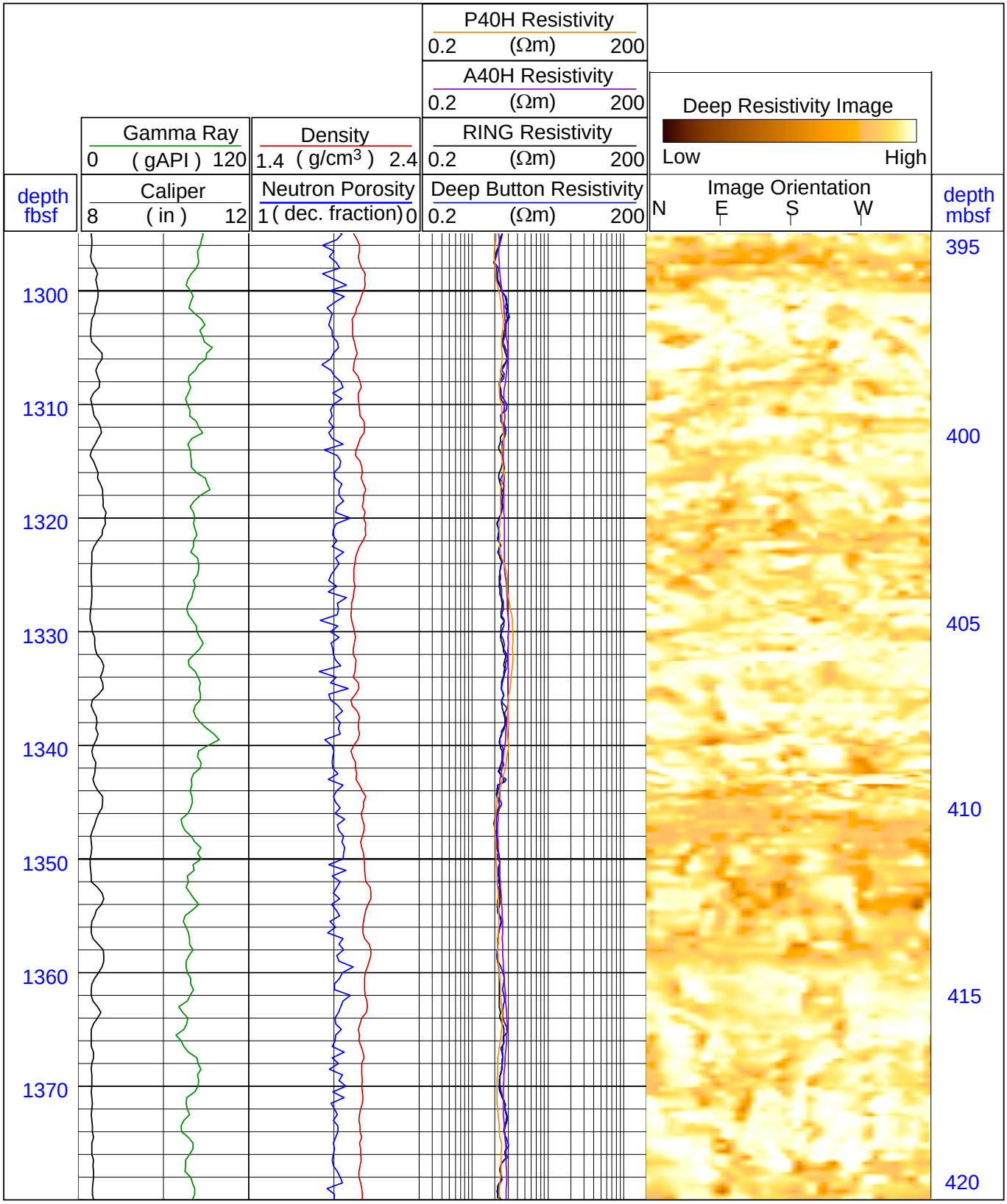

Figure F18: *Logs and LWD resistivity image from 1295 to 1380 fbsf in Hole AC 21-A, showing a possible gas hydrate-bearing section. Ring = Ring resistivity (geoVISION); P40H = Phase-shift resistivity at 2 MHz and a transmitter-receiver spacing of 40 inches (EcoScope); A40H = Attenuation resistivity measured at 2 MHz and a transmitter-receiver spacing of 40 inches (EcoScope).*

References

Collett, T.S., Boswell, R., Mrozewski, S., Guerin, G., Cook, A., Frye, M., Shedd, W., and McConnell, D., 2009. Gulf of Mexico Gas Hydrate Joint Industry Project Leg II — Operational Summary: Proceedings of the Drilling and Scientific Results of the 2009 Gulf of Mexico Gas Hydrate Joint Industry Project Leg II. http://www.netl.doe.gov/technologies/oil-gas/publications/Hydrates/2009Reports/OpSum.pdf

Frye, M., Shedd, W., Godfriaux, P., Collett, T.S., Lee, M., Boswell, R., Dufrene, R., 2009. Gulf of Mexico Gas Hydrate Joint Industry Project Leg II — Alaminos Canyon 21 Site Summary: Proceedings of the Drilling and Scientific Results of the 2009 Gulf of Mexico Gas Hydrate Joint Industry Project Leg II. http://www.netl.doe.gov/technologies/oil-gas/publications/Hydrates/2009Reports/AC 21SiteSum.pdf

Cook, A., Guerin, G., Mrozewski, S., Collett, T.S., Boswell, R., 2009. Gulf of Mexico Gas Hydrate Joint Industry Project Leg II — Walker Ridge 313 LWD Operations and Results: Proceedings of the Drilling and Scientific Results of the 2009 Gulf of Mexico Gas Hydrate Joint Industry Project Leg II. http://www.netl.doe.gov/technologies/oil-gas/publications/Hydrates/2009Reports/WR313LWDOps.pdf

Cook, A., Goldberg, D., and Kleinberg, R., 2008. Fracture-controllwed gas hydrate systems in the northern Gulf of Mexico. Marine and Petroleum Geology, 25, 932-941.

Guerin, G., Cook, A., Mrozewski, S., Collett, T.S., Boswell, R., 2009. Gulf of Mexico Gas Hydrate Joint Industry Project Leg II — Green Canyon 955 LWD Operations and Results: Proceedings of the Drilling and Scientific Results of the 2009 Gulf of Mexico Gas Hydrate Joint Industry Project Leg II. http://www.netl.doe.gov/technologies/oil-gas/publications/Hydrates/2009Reports/GC955LWDOps.pdf

Mrozewski, S., Guerin, G., Cook, A., Collett, T.S., Boswell, R., 2009. Gulf of Mexico Gas Hydrate Joint Industry Project Leg II — LWD Methods: Proceedings of the Drilling and Scientific Results of the 2009 Gulf of Mexico Gas Hydrate Joint Industry Project Leg II. http://www.netl.doe.gov/technologies/oil-gas/publications/Hydrates/2009Reports/LWDMethods.pdf